SAFETY ZONES OF QUALITY DURING DEEP DRAWING OF AXIS-SYMMETRICAL BLANKS

Nikola Nikolov*, Anguel Baltov*

A complex safety surface of the quality of deep drawn steel pieces is built on the basis of 45 numerical experiments. This surface is a combination of subsurfaces reflecting the effects of plastic strain localization and stability loss of the form change of circular blanks. The safety zone of quality is disposed below the safety surface. Two parameters of quality are proposed. Their high values lead to dispositions of drawing forces out of the safety surface of quality and to disturbance of quality, respectively. The results obtained for the safety zone and reported in this paper give an opportunity of estimation in advance phenomena as plastic strain localization and stability loss during the blank form changes. The safety surface of quality is given, and respective illustrative examples are presented.

Keywords : *deep drawing, safety zones of quality, plastic strain localization, stability of shape*

1. Introduction

The deep drawing process is one in between the production processes assuring high productiveness. For this reason, the question about the quality of produced pieces becomes essentially important. The requirements for the quality of sheet metal pieces produced by plastic forming must be assured during blank forming in advance at the stage design of technological processes. Here, some basic in between mandatory requirements will be discussed.

A) Requirement of strength – the failure criteria must not be achieved in the blank volume during blank forming, and local breaking must not be obtained [1].

B) Requirement of stability of the deformation process – local stability loss of the inside deformation process which leads to forming plastic localization bands must not be obtained. Such strips assist the forming of shear macro-cracks. This requirement is checked by respective criteria [2].

C) Requirement of stability of the change of blank form during the forming process. This requirement is also checked by corresponding criteria [3].

In present elaboration the requirements B and C are taken into consideration because in many cases the requirement A is not governing. The requirements have led to different criteria. These criteria form the limit plastic deformation regimes.

The diagrams obtained by tensile tests (Fig. 1) and corresponding analytical and experimental techniques are widely used in predicting the formability of metal sheets [4–8].

* Dr. N. Nikolov, prof. A. Baltov, DSc., Institute of Mechanics, Bulgarian Academy of Sciences, Acad. G. Bontchev Street, Block 4, 1113 Sofia, Bulgaria

In test procedures [4] for determination of the formability of sheet metal through tensile testing the main focus is the forming limit in plane strain state and getting a better understanding of the material behavior prior to and during localization and fracturing. Different simulations are performed in order to find appropriate design of the specimens prior to testing and performing various parameter studies.

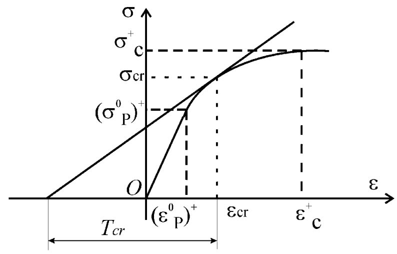

Fig.1: Stress-strain curve at tension

A yield function calibration involving three directional uniaxial and two plane strain tensile tests is proposed, satisfying results are demonstrated [5]. A Generalized Forming Limit Diagram which demonstrates significantly increasing forming limits through both normal compressive stresses and thickness shear is proposed. The forming limit, fracture limit and wrinkling limit diagrams are experimentally evaluated and compared for various interstitial-free (IF) steel sheets possessing thicknesses 0.6, 0.9, 1.2 and 1.6 mm. The suitability of steel sheets for press forming under different strain combinations is examined, and the tensile properties and formability parameters are correlated with the forming, fracture and wrinkling limit diagrams [6].

Since the blank holder forces [7] and friction conditions could often be restricting factors and reasons for low piece quality [8], a properly designed sheet metal forming process should give opportunity of respective adjustments. A weighted sum approach is used to derive a scalar measure of efficacy for the multi-criteria optimization taking into account wrinkling and fracture failures [9, 10].

The taking into account both the damage behavior and texture behavior is a reserve which helps in improvements of the predictions of material formability. Such a prediction of maximum strains and modeling damage evolution give opportunity to take decisions in the process design [11]. Another aspect taking part in the piece quality is the influence of crystal orientation on stress-strain state. A study on strain localization of BCC steel sheets is performed in [12]. The possibility to develop an optimum design system of the texture of high strength steel with better formability by using crystalline plasticity FE analysis is shown. FE analyses revealed that the crystal orientation fibers have close relations to the occurrence of failure in metal forming processes.

The die roundness radius is an geometrical parameter essential for the limit stress-strain states of blank, and unsuitably chosen values could lead to inapplicability of forming limit results to given processes. A qualitative analysis allowing understanding of the contact conditions on the die radii at sheet metal stamping processes shows the existence of distinct phases [13].

Investigating safety zones, it is useful to consider a type of plastically formed blanks for which an approach making more precise the conditions assuring the requirements pointed out could be given. That will permit determination in advance whether the geometrical sizes, blank material and forming loads are properly accepted to meet above requirements (A, B, C) during design of definite piece. For this purpose, the present paper suggests dimensionless parameters which describe relations between the geometrical sizes of blank and forming tool depending on the blank material. A space of events covering these dimensionless parameters and loading parameters is introduced. Two groups of criteria are proposed, and a safety zone of quality during blank forming is created. In order to estimate the process quality points identifying the blank forming state are searched in the space of events, and after a check on fall in the safety zone is performed.

Consequently, there exists a surface which is determined by the final qualitative forms of pieces during plastic deformation of corresponding blanks. The quality of given piece produced by cold sheet plastic deformation will be assured in the safety zone if the processing achieves but does not overcome the limit surface of forming. This approach is developed for structural elements in [1]. In the present elaboration, a method of construction of safety zones of the quality during deep drawing of circular steel blanks will be represented. Thereby, this approach is applied for the first time in a technological process of sheet metal forming.

2. Method of construction of safety zones of quality during deep drawing of axis-symmetrical blanks

2.1. Numerical simulation of deep drawing

In Fig. 2, the geometrical sizes of axis-symmetrical sheet metal blanks and loading scheme during a deep drawing step st are given, where: r_m is die roundness radius; R_p and r_p are the punch radius and punch roundness radius; q is specific blank holder pressure; D_Z^{st} is the blank contour diameter with the step st and $\varrho_1^{st} = D_\mathrm{Z}^{st}/2$ is the running size of the blank flange (blank contour) in each step.

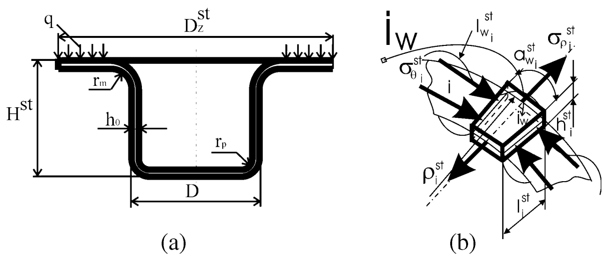

Fig.2: Scheme of the blank forming by deep drawing (a) with a blank flange element (b)

With the first step ($st = 1$) the blank diameter and radius follow the dependency $\varrho_1^1 = D_\mathrm{Z}^1/2$. H^{st} is a running drawing depth achieved with drawing force $P^{st} = P^{st}(t)$ at a moment $t = t(H^{st})$ or punch travel S^{st} both achieved before quality disturbance through appearance of plastic strain localization, blank flange waviness or blank breaking. Here, $H^{st} \leq H_\mathrm{f}$, and H_f is a given final blank height. That depends on the given piece configuration including some flange or not. The height H^{st} and punch travel S^{st} are equal i.e. $H^{st} = S^{st}$ until beginning the third geometrical stage of deep drawing when the blank radius ϱ_1^{st} becomes smaller than the sum of both the radii of die R_m and die roundness r_m.

During the simulation a blank with given initial diameter D_Z^0 and thickness h_0 is divided into m concentric ring elements (Fig. 2a). During each computational step st ($st = 1, 2, \ldots, L$) each element i ($i = 1, 2, \ldots, m$) has length l_i^{st}, thickness h_i^{st} and running radius ϱ_i^{st} (Fig. 2b). The forming process time is discretized in steps Δt^{st} (stages) corresponding to steps Δs^{st} of the punch travel S^{st}. Updated Lagrange's approach is applied. The displacements, strains and stresses of elements are computed in each step Δt^{st} starting from the data obtained in the previous step Δt^{st-1}. The infinitesimal increments of strain intensities $\mathrm{d}\varepsilon_i^{st}$ are substituted with finite increments $\Delta\varepsilon_i^{st}$. The initial non-deformed state of the blank is starting condition in the computations. The following boundary conditions are applied: in each step st the first flange element $i = 1$ must have assigned displacement depending on the punch step Δs^{st}; the last bottom element $i = m$ must have displacement approximately zero. In each computational stage the piece quality is controlled by the check of criteria for blank fracture, plastic strain localization and blank flange wrinkling. The drawing force P^{st} in each step is calculated according to:

$$P^{st} = 2\,\pi\,\sigma_{\varrho C}^{st}\,h_C^{st}\,\varrho_C^{st}\,\cos\varphi^{st}\ , \tag{1}$$

where (Fig. 2a), φ^{st} is the slope of conical blank part during the initial steps and takes values from 0 to $\pi/2$, and the subscript C assumes the number of first element of the conical part during treated step. C could take different number i according to the process development. The stress $\sigma_{\varrho C}^{st}$ is obtained according to the equations of Plastic flow theory [15].

2.2. Introducing dimensionless parameters characterizing the running change of blank form

Different dimensionless parameters of quality could be introduced reflecting the geometrical size variations with forming process development. Their choice is not a trivial procedure. In this elaboration two cases are taken into consideration.

Case (I), when:

$$\xi = \frac{H_\mathrm{f}}{r_\mathrm{m}} \quad \text{and} \quad \eta = \frac{D_\mathrm{Z}^0}{2\,h_0}\ . \tag{2a}$$

The parameters ξ and η do not depend on the process development.

Case (II), when:

$$\xi^{st} = \frac{H^{st}}{r_\mathrm{m}} \quad \text{and} \quad \eta^{st} = \frac{D_\mathrm{Z}^{st}}{2\,h_0} = \frac{\varrho_1^{st}}{h_0}\ . \tag{2b}$$

In this case, both the parameters H^{st} and D_Z^{st} depend on the process development. At each forming step during processing time such a choice of parameters makes possible to observe the change of geometrical blank parameters and to identify their respective limiting values if an indication for disturbance (Criteria B, C) of the piece quality appears.

The basic loading parameter is the drawing force on the punch $P(t)$. The clamping on the blank flange q is assumed to be fixed ($q = q_0 = \mathrm{const}$, Fig. 2). The space of introduced dimensionless parameters (P, ξ, η) is called space of the events.

In Fig. 3 with chosen (ξ, η) according to equation (2a) schemed by Case (I) or (2b) schemed by Case (II), a three-dimensional space of events is shown. The force P changes starting from initial moment t_0 until a moment t_f when a given final drawing depth H_f is achieved.

The point P_g denotes the value of force $P(t)$ achieved during the monotonically raising forming load which reaches the first surface safety for quality according to the criterion B or C. P_m denotes the maximum value of $P(t)$ reached during the deep drawing until the final depth H_f. The process is realizable keeping the quality if $P_\mathrm{m} \le P_\mathrm{g}$. If $P_\mathrm{m} > P_\mathrm{g}$ the process is technologically not acceptable.

Two different cases are discussed according to definitions (2a) and (2b), Fig. 3. In this figure $P_\mathrm{m}(1)$ and $P_\mathrm{m}(2)$ denote two possible alternative situations: $P_\mathrm{m}(1) < P_\mathrm{g}$ or $P_\mathrm{m}(2) > P_\mathrm{g}$

for the Case (I) and Case (II). Two surfaces safety for the quality are built by introduction of the criteria B and C in the simulation procedure. In Fig. 3, limit forces P_g forming such surfaces are shown for some particular examples.

The images of the loading paths are presented for both the Cases (I) and (II) taken into consideration. In the first case $P = P(t)$ changes vertically as a straight line, Fig. 3.

In the second case, the loading path curve depends on the changes of the step parameters H^{st} and D_Z^{st}, and $P = P(t, \xi, \eta)$. If the parameters ξ and η are assumed depending on the running state of the deep drawing process i.e. $\xi^{st} = \xi^{st}(P)$ and $\eta^{st} = \eta^{st}(P)$ then the process path will not be line as in Case I in Fig. 3. It will be a curve corresponding to the above dependencies, Case II in Fig. 3.

In the plane of states (ξ, η), the area which is technologically acceptable is defined by $\xi \in [\xi_1, \xi_2]$ and $\eta \in [\eta_1, \eta_2]$.

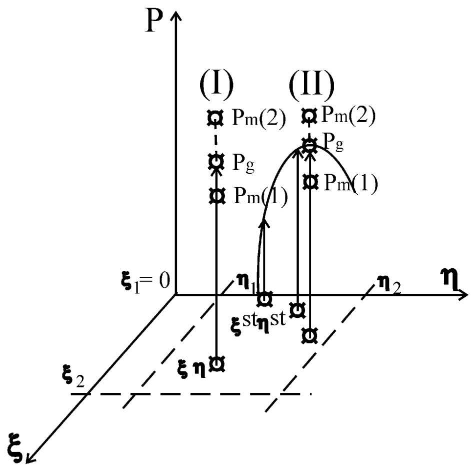

Fig.3: Space of events during deep drawing

2.3. Criteria for localization of plastic strain and for loss of stability of the blank flange forming

2.3.1. Localization of plastic strain

The critical plastic strains $\varepsilon_{\mathrm{cr}}$ leading to localization of plastic flow are obtained according to the Swift's approach [15]. The critical strains $\varepsilon_{\mathrm{cr}}$ are calculated through the expression (Fig. 1) :

$$\varepsilon_{\mathrm{cr}} = T_{\mathrm{cr}}\, n \ , \tag{3}$$

where n is the exponential index in eq. (4); σ_C^+ is the fracture limit at tension, ε_C^+ is respective limit strain; T_{cr} is the critical sub-tangent given in Fig. 1; $(\sigma_{\mathrm{p}}^0)^+$ and $(\varepsilon_{\mathrm{p}}^0)^+$ are the plastic yield limit and the corresponding limit strain at tension and A is material constant

$$\sigma^+ = (\sigma_{\mathrm{p}}^0)^+ + A\,[\varepsilon^+ - (\varepsilon_{\mathrm{p}}^0)^+]^n \ . \tag{4}$$

Two methods [2, 16] are used for check of criterion for plastic strain localization. The corresponding values are denoted by $T_{1\mathrm{cr}}$, $\varepsilon_{1\mathrm{cr}}$ and $T_{2\mathrm{cr}}$, $\varepsilon_{2\mathrm{cr}}$, respectively. T_{cr} and respective $\varepsilon_{\mathrm{cr}}$ are computed for each blank element i in each step st.

In the middle blank part, depending on the ratio m of the tangentional σ_θ to radial σ_ϱ stresses, the critical subtangent $T_{1\mathrm{cr}}$ [2] is:

$$T_{1\mathrm{cr}} = \sqrt{\frac{2\,(K+2)}{3}}\;\frac{\sqrt{(K+1)\,m^2 - 2\,K\,m + (K+1)}}{(K+1) - K\,m}\;, \tag{5}$$

where $m = m^{st}_{\varrho_i} = \sigma^{st}_{\theta_i}/\sigma^{st}_{\varrho_i}$ when $\sigma^{st}_{\varrho_i} > \sigma^{st}_{\theta_i}$ (Fig. 2b), and $m = m^{st}_{\theta_i} = \sigma^{st}_{\varrho_i}/\sigma^{st}_{\theta_i}$ when $\sigma^{st}_{\theta_i} > \sigma^{st}_{\varrho_i}$, K is the coefficient of transversal anisotropy. Close to the die roundness radius, $T_{1\mathrm{cr}}$ is [2]:

$$T_{1\mathrm{cr}} = \sqrt{\frac{2\,(K+2)}{3}}\;\frac{\sqrt{(K+1)\,m^2 - 2\,K\,m + (K+1)}}{K+1}\;, \tag{6}$$

Another condition of plastic strain localization is assumed as a controlling [16]. This condition takes into account the material's plastic anisotropy trough the form of the plastic surface. In this case $T_{\mathrm{cr}} = T_{2\mathrm{cr}}$:

$$T_{2\mathrm{cr}} = \frac{\left[C_1\,|1+m|^M + C_2\,|1-m|^M\right] C_3 \left[|1+P|^{\frac{M}{M-1}} + C_4\,|1-P|^{\frac{M}{M-1}}\right]^{\frac{M-1}{M}}}{(1+m\,P)\,C_1\,|1+m|^{M-2}\,(1+m) + (1-m\,P)\,C_2\,|1-m|^{M-2}\,(1-m)}\;. \tag{7}$$

In eq. (7) $M = K + 1$. The coefficients C_1, C_2, C_3 and C_4 are ratios of K and M. P is a ratio of m, M and C_1, C_2, C_3 and C_4. The corresponding expressions are given in [16].

2.3.2. Loss of the stability of blank flange forming

The check on loss of the stability of blank flange forming is accomplished through a criterion given in [3] and precised in [17]. In element i (Fig. 2), the state critical for waviness is defined by the work of internal forces, work of the surface forces and work of the clamping forces.

According to the pointed out criterion, the blank flange elements i are divided into sector parts i_w assuming forms similar to rectangular (Fig. 2b), and it is taken into account that during deep drawing such a part is loaded at pressure and tension along the axes. The criterion for the loss of stability in the stage st is:

$$h^{st}_i \le h^{st}_{\mathrm{cr}_i}\;, \tag{8}$$

where $h^{st}_{\mathrm{cr}_i}$ is computed by the relative critical thickness:

$$h'^{st}_{\mathrm{cr}_i} = \frac{h^{st}_{\mathrm{cr}_i}}{2\,r_0} = \frac{h^{st}_{\mathrm{cr}_i}}{2\,l^{st}_i}\,(r^{st}_n - m_1)\;. \tag{9}$$

In eq. (9), $r^{st}_n = 2\,\varrho^{st}_1/D^0_\mathrm{Z}$ is ratio of the running blank contour to the initial, and $m_1 = 2\,R_\mathrm{p}/D^0_\mathrm{Z}$ is the deep drawing coefficient. The sizes of element i_w formed as a part between two radial sections of a ring element i are l^{st}_i and $a^{st}_{\mathrm{w}_i} = l^{st}_{\mathrm{w}_i}/m^{st}_\mathrm{w}$ (Fig. 2b), where $l^{st}_{\mathrm{w}_i}$ is the curve-linear length of the blank ring element i in the treated step st and m^{st}_w is number of waves. More details are given in [3, 17].

3. Defining the limit surfaces and safety zone of quality

The defining of the limit surfaces corresponding to the Criteria B, C (Section 1) is performed by identification of points P_{g} belonging to them. That is accomplished trough numerical experiments carried out to detect respective critical for quality deep drawing forces P_{g} under precise values of ξ, η and clamping $q = \mathrm{const}$ (Fig. 3). The points obtained in this way are approximated by surface (Fig. 4).

The searched safety zone of quality of pieces obtained by deep drawing appears below this surface. Numerical experiments are performed by a simulation of deep drawing process according to Approximate Discrete Method (Section 2.1). The simulation gives opportunity of taking into account the influence of material's anisotropy, material's resistance at tension and pressure and strain rate [14].

An illustration of application of the method is presented. The blank material is a low-carbon steel with hardening curve at tension described by equation $\sigma = 530\,\varepsilon^{0.24}$ [15]. The transversal anisotropy coefficient is 1.7, and coefficient of different resistance is 1.18 . In 45 numerical experiments, the initial blank diameter D_{Z}^{0} and initial blank thickness h_0 are variable as parameters of the piece, and the die roundness radius r_m is variable as a parameter of the forming process. The levels of parameter changes are given in Table 1.

Parameters of:			Characteristics of:	
piece		forming	criteria	forming
D_{Z}^{0} [mm]	h_0 [mm]	r_{m} [mm]	B; C [mm]	load/deformation
106; 102; 98; 94; 90	0.5; 1.5; 2.5	2, 6, 10	$\varepsilon_{1\mathrm{cr}}$; $\varepsilon_{2\mathrm{cr}}$; h_{cr}	P^{st}; σ_i; ε_i; h_i

Tab.1: Parameters of deep drawing

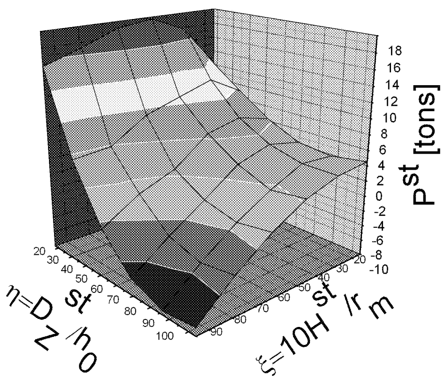

Fig.4: Safety zone of quality during deep drawing of axis-symmetrical low-carbon steel blanks

During each experiment the next characteristics are detected, Table 1 : maximal critical for quality drawing forces $P^{st} \equiv P_{\mathrm{g}}$, minimal critical blank thickness h_{cr} below which flange waviness appears and two minimal critical strains $\varepsilon_{1\mathrm{cr}}$ and $\varepsilon_{2\mathrm{cr}}$ computed according to two methods (Section 2.3.1, eq. 5–7), their overcoming lead to localization of plastic strains and obtaining non-qualitative peace.

During simulations it was established that the criteria B or C are fulfilled before strength criterion A. For this reason criteria B and C are only applied during composing safety surface. The disturbance of quality because of the appearance of localization is established in 20 processes, the respective critical drawing forces P_g definite a limit surface of plastic localization. The disturbance of quality because of the appearance of flange waviness is observed in 21 processes. Both the effects of localization and waviness are established in 13 processes. The obtained forces P_g define the corresponding surfaces. The flange waviness firstly appears mainly in the thinnest blanks having thickness 0.5 mm, and by deep drawing with the three die roundness radii. The plastic flow localization firstly appears in some of the blanks having mean thickness of 1.5 mm with deep drawing using the minimal die roundness radius 2 mm.

The limiting forces P_g are identified for 26 processes according to Criteria B and C. The common limiting surface safety for the quality is formed from the lesser value P_g obtained through any one in between both the criteria for each process (Fig. 4).

4. Numerical examples and application of the safety zone of quality

Five numerical examples are presented as illustrations of the proposed method. The deep drawing of low-carbon steel 08 is considered in them. The steel has yield stress limit $\sigma_S = 195$ MPa and ultimate tension stress limit $\sigma_B = 320$ MPa. All the blanks have constant diameters $D_Z = 100$ mm. The blank thickness is variable from 1 mm in Examples 1, 4 and 5, to 2 mm in Example 2, and to 1.5 mm in Example 3. The die roundness radius is changed from 8 mm in Examples 1, 2 and 3, to 10 mm in Example 4, and to 3 mm in Example 5. These variations aim to demonstrate the changes of both the parameters ξ and η depending on the forming process and their disposition with respect to the safety surface (Fig. 6).

High values of the first parameter are obtained with large punch travels and low die roundness radii (eq. 2). At the same time, that leads to significant possibilities of plastic strain localization and blank breaking since the large punch travel is related to high deformation ratio, and small radius leads to high radial stresses which may cause localization.

High values of the second parameter could be obtained with large running blank radii and small blank thicknesses. The large radius leads to high radial and circumferential stresses and possibility of localization and waviness. The small thicknesses coupled with that increase the possibility of obtaining a non-qualitative piece.

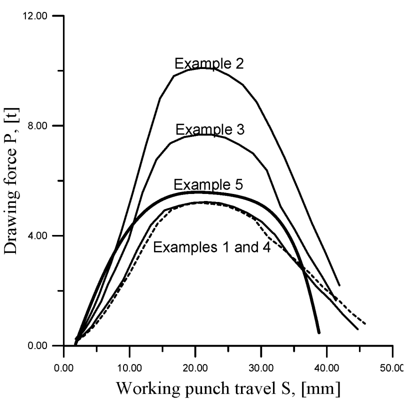

Fig.5: Diagrams 'Drawing Force P – Punch Travel S' obtained by numerical examples

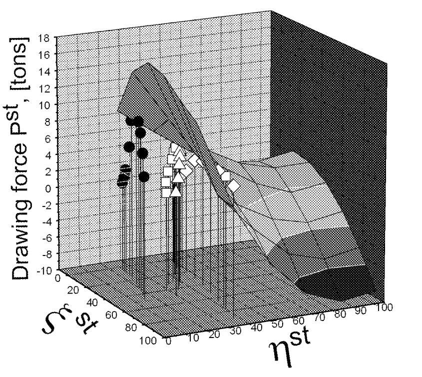

Fig.6: Disposition of the numerical examples (Fig. 5) in the space of events

It is obviously from the above, that the high values of both the parameters lead to reaching the limit regimes, and opposite – the low values could assure the production of more qualitative piece with lower possibility of plastic localization and blank flange waviness. The values of both the parameters could be directly obtained from the design task of piece.

Example 1. Deep drawing of steel blank possessing diameter 100 mm and thickness 1mm with punch diameter 50 mm, punch roundness radius 5 mm, die roundness radius 8 mm, gap between punch and die 0.6 mm, specific clamping 2 MPa. The corresponding criteria ξ and η with maximal drawing force 5.227×10^4 N, are $\xi = 10\, S^{st}/r_{\mathrm{m}} = 10\times21.63/8 = 27.03$ and $\eta = D^{st}_{Z\Phi}/2\, h_0 = 84.02/2 = 42.01$, where S^{st} and $D^{st}_{Z\Phi}$ are the running punch travel and running blank contour under the maximal drawing force.

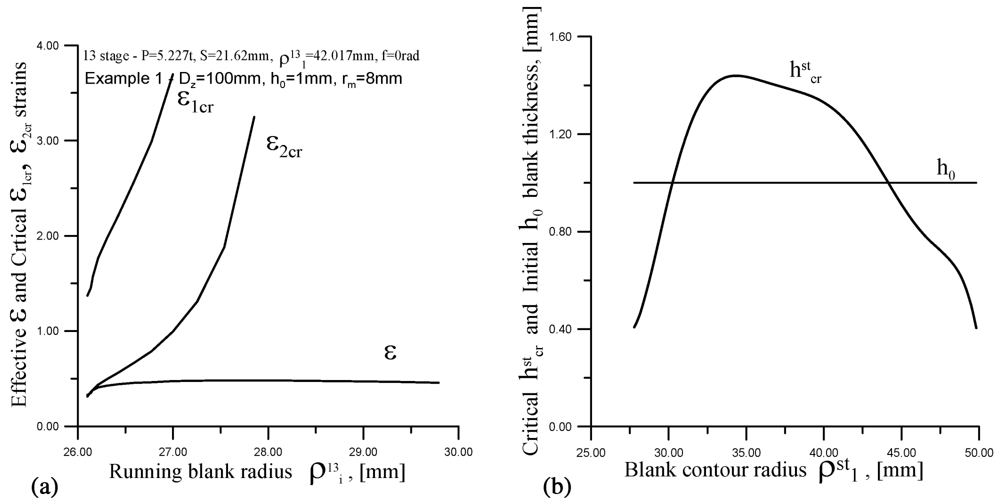

Fig. 7: Critical strain (a) and thickness (b) in Example 1

In Figs 6 and 7, the points determining this deep drawing regime are placed below and close to the limiting safety surface of quality. This demonstrates that by these discussed deep drawing parameters an effect in between both the plastic localization and flange waviness could be obtained and that will destroy the quality of formed piece. The numerical simulation of this process shows that with maximum drawing force 5.227×10^4 N, obtained under punch travel 21.63 mm and running diameter of blank contour 84 mm. According to the second criterion the plastic strain localization will appear in the area of the just formed blank wall (Fig. 6 and 7a) because the effective strains are equal to the critical. Moreover, Fig. 7b shows that a blank with such thickness and diameter could obtain loss of stability of the form under running diameter of blank contour 86 mm. In Fig. 6 it is seen that there exist few variants of change of both the criteria with aim shifting the drawing regime in the safety zone. The next examples demonstrate such possibilities.

Example 2. An increase of the blank thickness to 2 mm under the same other process parameters leads to criteria $\xi = 10\, H/r_{\mathrm{m}} = 10\times20.91/8 = 26.13$ and $\eta = D^{st}_{Z\Phi}/2\, h_0 = 85.16/4 = 21.29$ with drawing force 10.1×10^4 N. The corresponding point which determinates the deep drawing regime in the space of events appears in the safety zone admissible technologically. In Fig. 8a and b the results from the numerical simulation show strains below the critical according to both the criteria (eq. 5–7) and critical blank thickness about 1.4 mm with running blank contour radius about 35 mm (eq. 8 and 9).

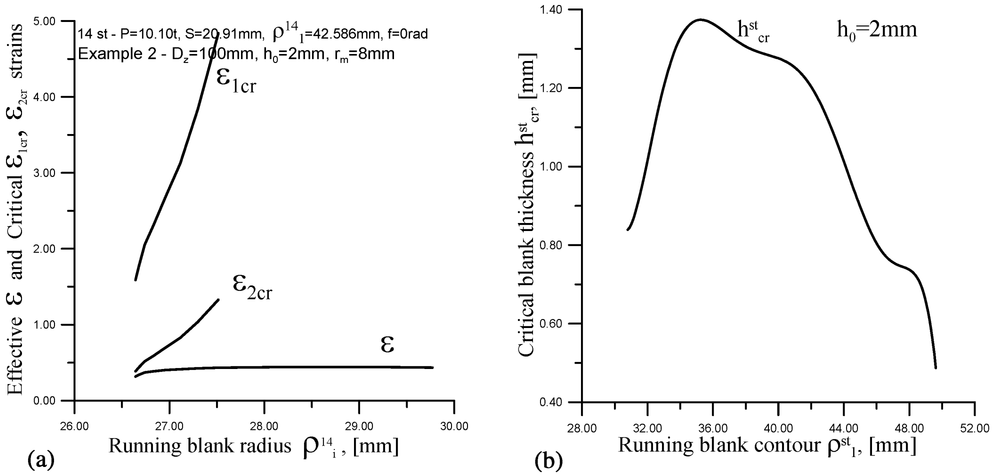

Fig.8: Critical strain (a) and thickness (b) in Example 2

Example 3. With blank thickness 1.5 mm and the same others process parameters as in Example 2, the criteria ξ and η have values $\xi = 10\,H/r_{\mathrm{m}} = 10\times22.47/8 = 28.08$ and $\eta = D^{st}_{\mathrm{Z\Phi}}/2\,h_0 = 83.178/2\times1.5 = 27.7$ obtained under maximal drawing force 7.676×10^4 N. The corresponded point determining the drawing regime in the space of events appears close to the safety surface (Fig. 6). The respective results obtained by the numerical simulation and given in Fig. 9a and b show values of strains and blank thickness close to the critical but below them.

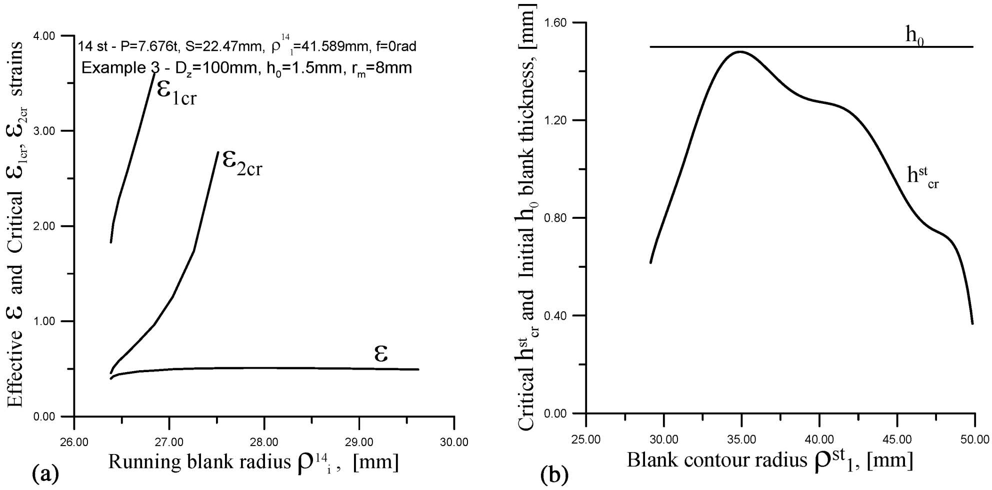

Fig.9: Critical strain (a) and thickness (b) in Example 3

Example 4. Under the initial conditions of Example 1, changing the die roundness radius from 8 to 10 mm and under the same others process parameters the criteria ξ and η are $\xi = 10\,H/r_{\mathrm{m}} = 10\times20.58/10 = 20.58$ and $\eta = D^{st}_{\mathrm{Z\Phi}}/2\,h_0 = 885.76/2 = 42.73$. Maximal drawing force is 5.198×10^4 N, and the deep drawing regime appears below and close to the safety surface given in Fig. 6.

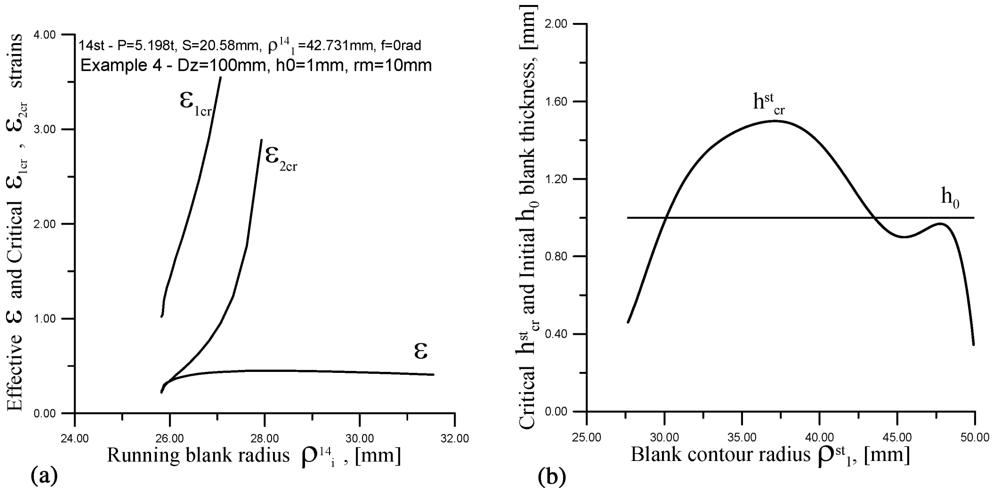

Fig.10: Critical strain (a) and thickness (b) in Example 4

Example 5. Under the initial conditions of Example 1, changing the die roundness radius from 8 to 3 mm and under the same values of the others process parameters, the critical ξ and η have values $\xi = 10\,H/r_{\rm m} = 10{\times}22/3 = 73.3$ and $\eta = D^{st}_{\rm Z\Phi}/2\,h_0 = 81.34/2{\times}1 = 40.67$. The maximal drawing force is $5.63{\times}10^4$ N and the points corresponding to the deep drawing regime appear significantly over the safety surface and outside safety zone of quality, Fig. 6. The detailed results obtained by the numerical simulation show clearly the same situation, Fig. 11a and b.

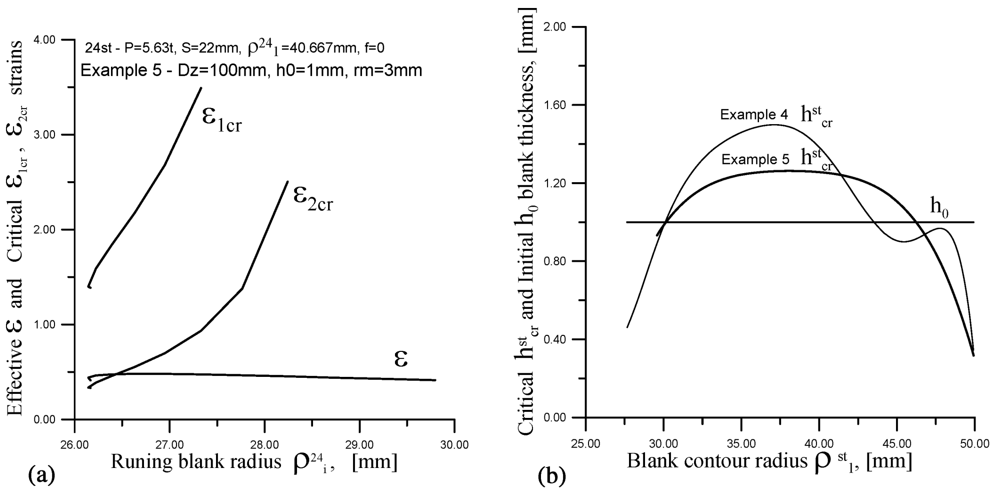

Fig.11: Critical strain (a) and thickness (b) in Example 5

5. Conclusions

The thickness of the blanks made of low-carbon steel is varied from 0.5 mm to 1.5 and 2.5 mm (Table 1) under five levels of blank diameter from 106 to 90 mm with step 4 mm. The die roundness radius is varied from 2 mm to 6 and 10 mm. These changes of pointed out parameters practically assure observations of material's behavior in the most applicable technological range of the deep drawing process. During the plastic blank forming the strain intensity and blank thickness change are established and compared to critical strains $\varepsilon_{1\mathrm{cr}}^{st}$, $\varepsilon_{2\mathrm{cr}}^{st}$ and critical thickness h_{cr}^{st}. The drawing forces P_{g}, corresponded to them and critical for piece quality, form the limiting safety surface of piece quality. The possibility of quality disturbance is predicted in this way.

It is established (Section 3, Figs 6, 8–12) that the localization of plastic flow is firstly observed with some blanks possessing mean thickness (of 1.5 mm in the pointed out interval) during the forming with die roundness radius 2 mm. It is also established that flange waviness appears firstly with thinnest blanks (having thickness 0.5 mm) during deep drawing through the three die roundness radii, and after that with the same blanks the plastic localization appears.

There exist many empirical formulas for calculation of drawing force [18]. The expressions describe the radial stresses and reflect the effects of die and punch roundness radii, blank thickness, yield and strength limits of material, friction coefficient, clamping and etc. But they do not give opportunities to make conclusions about appearance of phenomena disturbing the piece quality. The results obtained for the safety surface and reported in this paper give an opportunity to estimate in advance such phenomena as early as possible at levels forming conception and design of piece.

The proposed method of the construction of safety surface of the piece quality during deep drawing of low-carbon steel blanks could be successfully applied for others conventional metallic materials as aluminum, copper, brass and etc.

References

[1] Baltov A., Alexandrov A., Miltchev E.: Safety zones for inelastic structures under impulsive loading, Eng. Mechanics 1, (2001), 23

[2] Ruzanov F.I.: Stability of the Deep Drawing Process during Plastic Forming of Anisotropic Metal, Forging-Stamping Production 4, (1967), 19 (in Russian)

[3] Golovlev V.D.: Calculations of sheet stamping processes, Stability of the forming of thin sheet metal, 1st ed., Machine-Building 1974, Moscow (in Russian)

[4] Holmberg S., Enquist B., Thilderkvist P.: Evaluation of sheet metal formability by tensile tests, J. of Mater. Process. Technology 145, (2004), 72

[5] Aretz H., Hopperstad O.S., Lademo O.-G.: Yield function calibration for orthotropic sheet metals based on uniaxial and plane strain tensile tests J. of Mater. Process. Technology 186, (2007), 221

[6] Allwood J.M., Shouler D.R.: Generalised forming limit diagrams showing increased forming limits with nonplanar stress states, Int. J. of Plasticity 25, (2009), 1207

[7] Narayanasamy R., Narayanan C.S.: Forming, fracture and wrinkling limit diagram for IF steel sheets of different thickness, Materials & Design 29, (2008), 1467

[8] Donglai W., Zhenshan C., Jun C.: Optimization and tolerance prediction of sheet metal forming process using response surface model, Comput. Mater. Science 42, (2008), 228

[9] Krishnan N., Cao J.: Estimation of Optimal Blank Holder Force Trajectories in Segmented Binders Using an ARMA Model, Trans. ASME, J. of Manuf. Sci. and Eng., November, (2003), 763

[10] Zhang W., Shivpuri R.: Probabilistic design of aluminum sheet drawing for reduced risk of wrinkling and fracture, Reliability Engineering and System Safety 94, (2009), 152

[11] Elgueta M.: Ductile damage analysis of sheet metal forming, J. Mater. of Process. Technology, 121, (2002), 148

[12] Xie C.L., Nakamachi E.: Investigations of the formability of BCC steel sheets by using crystalline plasticity finite element analysis, Materials & Design 23, (2002), 59
[13] Pereira M.P., Duncan J.L., Yanc W., Rolfe B.F.: Contact pressure evolution at the die radius in sheet metal stamping, J. of Mater. Process. Technology 209, (2009), 3532
[14] Nikolov N., Baltov A.: Influence of Material Senstitvity to Stress State on The Optimal Design of Deep Drawing Technological Processes, Eng. Mechanics 6, (2007), 373
[15] Nikolov, N., Loss of stability of the deformation process during deep drawing technological process, J. of Theor. and Appl. Mechanics 2, (2006), 31
[16] Esche S.K., Shivpuri R.: A Consistent Criterion for Diffuse Necking in Sheet Metals Using Hill's 1979 Yield Surface, Trans. ASME, J. of Eng. Mat. and Technology, April, (1998), 177
[17] Nikolov N.: Loss of stability of the blank forming process during deep drawing technological process, J. of Mater. Sci. and Technology 3, (2002), 12
[18] Unksov E.P., Johnson W., Kolmogorov V.L.: Theory of Plastic Deformation, 1st ed., Machine-Building 1983, Moscow

Received in editor's office: may 30, 2009
Approved for publishing: October 19, 2009